Decentralized Secondary Frequency Control in an Optimized Diesel PV Hybrid System

Alice Vieira Turnell[1],
Peter-Philipp Schierhorn, Daniel Masendorf
Energynautics GmbH
Darmstadt, Germany
Email: p.schierhorn@energynautics.com

Kateryna Morozovska
School of Electrical Engineering and
Computer Science
KTH Royal Institute of Technology
Stockholm, Sweden

***Abstract*—This research aims at investigating if a diesel-based isolated electrical system can be optimized by integrating a high share of solar photovoltaic (PV) generation and if the frequency stability of such system can be improved by including the PV participation in frequency regulation. A case study is developed in order to explore an island's expansion of the installed generating capacity and its optimization. This study uses the tool HOMER Energy Pro to solve the optimization problem and PowerFactory to verify the frequency stability of the proposed system. The PV integration allows for a reduction of diesel fuel consumption, emissions and generation costs. Additionally, in high PV penetration scenarios, the reduced inertia in such systems can lead to high frequency deviations that may trip the system protection. The study demonstrates that the instantaneous frequency deviation after a load and generation imbalance can be reduced by designing the PVs to operate with an allocated reserve and a decentralized time-based secondary frequency control. The system remained stable under different disturbance scenarios with high PV penetration and reduced available inertia, indicating that high PV integration is economically and technically feasible in a small island system.**

I. Introduction

The Indonesian government has set a renewable generation target of 23% of renewables in produced electricity by 2025. Indonesia comprises several islands, many of which are isolated and with electrical systems relying fully on diesel generators, resulting in high generation costs. Integrating a high share of renewable generation in such systems can reduce the generation cost, contribute to achieving the national target and to reducing greenhouse gas emissions.
Inverter based generators, such as solar photovoltaic (PV) and wind power, display characteristics inherently different from synchronous generators. The addition of high capacities of such generation may significantly impact the technical characteristics of the system and the operational procedures required to retain stable and secure supply. Frequency control is one of the key parameters impacted by the introduction of high shares of PV and is thus the subject of this paper. PVs are currently capable of frequency regulation using droop methods and grid codes are starting to require such participation, through operation reference points set by the transmission system operator [1]. The fast operation of inverter based generation technologies has the potential to improve the systems stability through the participation of such technologies in frequency regulation.

[1]The author performed the research as part of the master thesis in KTH. The research was conducted at Energynautics GmbH.

II. Methodology

The occurrence of disturbances in the active power balance of a system immediately triggers the kinetic energy stored in the rotating masses of machines, this phase is called the Inertial Frequency Response (IFR), which contributes to reducing the Instantaneous Frequency Deviation (IFD). The IFD should not exceed the maximum permissible limit as it may trigger protection systems, causing further system instabilities which can lead to black outs. Frequency controllers then act through the adjustment of the generators production in order to stabilize the frequency variation and return it to the systems nominal value. An increase in the system's load will reduce the system's frequency and, in order to adjust their production upwards, the generators participating in frequency regulation must operate with a reserve capacity. Frequency Containment Reserve (FCR), also named primary frequency control, is activated within seconds based on a pre-defined frequency droop in order to stabilize the system frequency and is an automatic response, commonly from the mechanical speed governor control of rotating generators. Frequency Restoration Reserve (FRR), also named secondary frequency control, is activated within a few minutes in order to regulate the frequency error to zero and replace the activated FCR. Whereas the FRR in larger systems are usually automatically dispatched, small islands may rely on manual adjustments. In remote islands, a less reliable channel could compromise the communication network used for an automatic centralized dispatch. Decentralized methods, in which each participating generating unit has a local secondary frequency controller, represent an alternative strategy for systems with unreliable communication channels, in order to avoid further instabilities caused by communication delays or interruptions in channels which are used for the centralized generation dispatch.

A. Case description

An Indonesian island was selected for a large-scale renewable integration scenario analysis. The island, with 13000 inhabitants and 0,8 MW peak consumption, is supplied by two diesel generators during 12 hours per day, and has a (high) cost of electricity estimated as 0,21-0,30 EUR/kWh. In the first step of this case study, an optimization problem is structured and solved using the island's specific technical and economic parameters in order to obtain the optimal capacity expansion plan for the island. Afterwards, the optimal solution is further analyzed using dynamic simulations in

order to verify the systems frequency stability under different scenarios in which the PVs are contributing to frequency regulation.

B. Optimization of the capacity expansion

1) Optimization Parameters: The renewable energy potential in the island region can be analyzed using data available in [2]. Total mean capacity factors of 16,5% and 2,90% were estimated for solar[1] and wind generation plants in the island, respectively. The low capacity factor observed for wind energy makes the installation of wind turbines in the island economically unfeasible. Therefore, diesel generators (existing and new), PV and battery systems are considered in the optimization problem.

The load was scaled based on the growth forecast of the island's population. A 20% load increase per year was considered, which would result in a consumption of only half the Indonesian average by the year 2025. A derating factor of 80% was included for the PV system, approximated from the 0,77 suggested by NREL's PVWatts [3], with an additional 1% loss per year. The parameters of the diesel generators were the same of the existing generators on the island, available in the manufacturer's equipment datasheet, and with a minimum load ration of 10% and lifetime of 25 years. This lifetime considers an overhauling every 2-3 years for small generators, which also contributes to the high cost of electricity.

Research was conducted on current and forecasted costs for PVs, Li Ion battery systems and diesel generators. The transportation cost of the existing generators in the island (1,47 EUR/kg) was included in the capital cost of the components in order to obtain values specifically for the island. The economic parameters used are listed in Table I. The capital cost forecast, excluding transportation costs, considers a yearly reduction of 9%[4] on equipment cost (67% of total) for the PV and battery inverter and 4,5%[5] on equipment cost (74% of total) for the batteries, as well as a -1% on the remaining percentage (installation costs)[6].

TABLE I
CAPITAL AND OPERATIONAL COSTS OF THE SYSTEM COMPONENTS.

	2018 Capital Cost [EUR/kW]	Operation and Maintenance Cost
PV [2]	990	12,16 EUR/kW,year
Battery Inverter[3]	429	0
Batteries (Li Ion) [2]	283,15 EUR/kWh	5,7 EUR/kWh,year
Diesel Generator [4]	243,24	0,0097 EUR/kW,hour 15000 EUR/year 0,589 EUR/L of fuel

2) Optimization Constraints: The constraint used were: no capacity shortage allowed, in order to guarantee that every peak load can be met by the generation installed capacity; at least one of the diesel generation must be running at all times; the minimum renewable fraction to be achieved, corresponding to the annual share of the generation supplied to the load that was originated from renewable energy, corresponds to the Indonesian target for the year 2025; the operating reserve as a percentage of the solar power was defined based on the irradiance variations of up to 80% within a minute, obtained from the irradiance measurements of a location in the island's vicinity.

[1]No tracking, zero tilt and 10% system losses were considered.
[2]Costs calculated based on data from [6].
[3]Costs from the quotation of an existing PV plant in the island's vicinity.
[4]Costs obtained from existing units on the island.

C. PV Frequency Control Strategy

The designed PV control model is based on the method proposed by [7], modified for a grid-following inverter with an allocated reserve level, as well as in a previous model made by Energynautics GmbH, which consists on an adaptation of the generic three-phase PV model. In Table II, a comparison is made between the main features of each model/method. Compared to the previous model by Energynautics GmbH and to the method proposed by [7], the proposed model has the main advantages of:

- improved system's frequency response to under-frequency events, by operating PVs with a reserve as a fraction of the Maximum Power Point (MPP).
- differentiated active power sharing between PVs and diesel generators during the over and under-frequency regulation process, through different over- and under-frequency control parameter settings of PV units.
- maximized total PV output (maintaining the reserve level) in the active power sharing between PVs and diesel generators after the restoration of the frequency.

TABLE II
COMPARISON OF FEATURES FROM DIFFERENT PV FREQUENCY CONTROL STRATEGIES.

	Energy-nautics Model	Method in [7]	Proposed Model
Over-frequency reaction	Yes	Yes	Yes
Reserve allocation and under-frequency reaction	No	No	Yes
Secondary frequency control without communications	No	Yes	Yes
Default operation point	MPP	MPP	(MPP-reserve)
Different over and under-frequency droop parameters	No	No	Yes
Inverter model (Grid Forming -GF, or grid following -PQ)	PQ	GF	PQ
Parameters adjusted for a small diesel-PV system	No	No	Yes

An active power reference is calculated in the controller that will lead to the regulation of the inverter's active power output, allowing the PV contribution to frequency regulation. The frequency set-point proposed in [7] is modified to an active power set-point $P_{setpoint}$, given by:

$$P_{setpoint} = P_{meas} - P_{droop} + \delta_P \tag{1}$$

where P_{meas} is the PV system measured active power output, δ_P is the secondary control term added in order to correct the steady-state error introduced by the primary control [7] and P_{droop} is the droop contribution, given by Equation 2.

$$P_{droop} = \frac{1}{K_{droop}} \Delta\omega \tag{2}$$

Where $\Delta\omega$ is the difference between the measured and nominal frequency; K_{droop} is the droop coefficient. Different coefficients are set for under and over-frequency events. The droop contribution is activated in the control strategy if the measured frequency leaves the frequency dead-band region. The term P_{droop} will be zero once the frequency is restored to within the hysteresis dead-band region.

Although the operation of the frequency control is decentralized, the droop coefficients must be selected having a global knowledge of the system to ensure active power sharing [8]. A study performed by [9] indicated that when PVs are configured with steeper droop curves, the nadir frequency reduces at the cost of higher oscillations, especially when the amount of PVs contributing to frequency regulation is high. Additionally, a frequency dead-band must be used in order to avoid excessive actions from the governor control due to small variations in frequency during normal operation.

The secondary control regulation is performed by the active power increment δ_P, expressed as per the transfer function δ proposed by [7] and represented in the Laplace domain in Equation 3, with the gains selected to reflect a power reference contribution.

$$\delta = \begin{cases} \frac{k_1}{s+k\ k_1}\ (\omega_0 - \omega), & k\,(t) > 0 \\ C, & k\,(t) = 0. \end{cases} \tag{3}$$

The time-dependent control scheme has been proposed in [7], in order to overcome the trade-off for which a faster frequency response yields a higher error of a P controller. The controller will switch between a filtered proportional controller and an integral controller, based on the control gain $k(t)$, as per Figure 1. In case of a frequency event, the control process time counter will start, with the secondary controller gain $k(t)$ as k_{max}, constant during the time interval Δ_{ct} and linearly decreasing to zero during the time interval Δ_{ramp}. For values of $k(t)$ equal to zero, δ will assume a constant value C, which corresponds to the last value calculated. The integral control gain k_1 is chosen based on the transfer function of the system and the desired location of the closed-loped poles. The term δ_P is activated in parallel with the droop contribution, once the measured frequency leaves the frequency dead-band region. The frequency event triggers the time-based secondary control strategy, in which the term δ_P will be updated as long as the frequency regulation process is active.

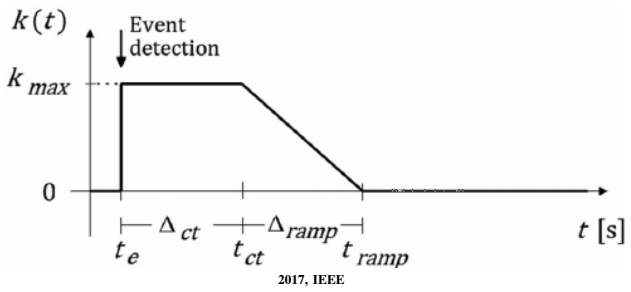

Fig. 1. Time-dependent controller gain after event detection. Source: [20].

Whilst the frequency is being regulated, which occurs after the event triggers the time-based control and during the control process time, the PV set-point has the maximum limit of the available MPP, therefore allowing the PV system to use its allocated reserve to increase the active power output during under-frequency events.

At the end of the control time, if the frequency has not been restored to within the frequency hysteresis dead-band, the control timer is restarted, restarting the control process. Otherwise, Equation 1 is replaced by Equation 4, limiting the maximum PV output to the reserve level.

$$P_{setpoint} = P_{reserve} \tag{4}$$

1) Implementation: The island's 2025 grid is modelled in PowerFactory using the results for the optimal installed capacity and data from the current electrical system on the island. The model includes existing and new diesel generators, the PV plants, the 20kV grid, medium voltage (MV) to low voltage (LV) transformers and loads as aggregated loads in the LV side of the transformers.

A total of eight locations were selected for PV plant installations, based on proximity to large load centres and at the end of long lines. Distributing the installed capacity of the PVs in the island contributes to: reduced power losses on the lines due to the generation proximity with the loads, improved system stability due to solar irradiance variations (cloud movement) affecting less PV plants simultaneously, improved voltage along the feeders, and increased system reliability by reducing the probability of disconnecting multiple generating units.

The assumptions made and parameter values used as inputs to the PowerFactory simulations are:

- all panels within the same PV plant receive the same solar irradiance values and constant temperature (25°C);
- the load is kept constant at the maximum 2025 forecasted daytime demand (1,8 MW);
- the PV module current, voltage and temperature correction parameters were those defined in the Powerfactory generic model of a 3-phase, 50Hz PV system. Parameters for the diesel generators were sourced from the manufacturer for the model installed in the island;
- a sensitivity analysis was performed to select the control parameters which result in the best frequency response for the case study, listed in Table III. This selection is a compromise between controller speed and the system oscillations;
- all PV plants have equal installed capacity and droop coefficients.

TABLE III
CONTROL PARAMETERS.

Parameter	Selected Value
Frequency deadband	[49,5; 50,5] Hz
Control Gains	Kmax: 0,2; Ki: 90
Control times	Δ_{ct}: 3 and Δ_{ramp} 5 seconds
Droop Coefficients	Under-frequency: 3%; Over-frequency: 5%

III. RESULTS AND DISCUSSION

A. Optimization of installed generation capacity

The optimal solution obtained for the 2025 system with and without renewable sources for the 20% load increase scenario can be found in Table IV. The optimal solution

corresponds to 3113 kW of PV systems, 675 kWh of Li ion batteries, 493 kW of battery inverter and 4 diesel generators of 656kW (prime rating), out of which two correspond to the already installed units. Regarding the battery technology, the optimal solution always selected the Li ion over lead acid. This is due to the higher lifespan and performance of Li ion batteries, despite an initially higher capital cost.

TABLE IV
OPTIMIZATION RESULTS.

	Scenario with renewables	Diesel-only Scenario	
	2025	2017	2025
Optimal Installed Capacity:			
Diesel generator [kW]	2624	1312	3280
PV System [kW]	3113	-	-
Li ion [kWh]	675	-	-
Battery Inverter [kW]	493	-	-
Minimum renewable fraction [%]	24,35	0	0
PV production curtailed [%]	22	-	-
LCOE [EUR/kWh]	0,140	0,21 [1]	0,167
Fuel Consumption [L/year]	2567	1032 [2]	3399

The renewable fraction target of 23% by 2025 is met and exceeded in the simulation, reaching 24,35% by 2025. The simulation for year 2025 was optimized with and without the constraint of 23%. The solution obtained was the same in both simulations, indicating that the expected cost parameters of the components led to an optimal installed capacity which meets the target independently of the constraint.
The LCOE considers the average cost per kWh of useful energy produced and is obtained as 0,14 EUR/kWh for the optimal solution, representing a 33% reduction from the 2017 cost.
If the 2025 load is supplied using diesel generators only, 5 units would be necessary and would yield a LCOE of 0,167 EUR/kWh, 19,3% higher than with PV units in the system. The total fuel cost is a major cause of this high LCOE, with a fuel consumption (and emissions) 32% higher in the diesel-only scenario. The LCOE of the 2017 system is shown in Table IV for comparison, and corresponds to the cost with less efficient generators operating in the system.
The optimal installed capacity of PV is larger than would be required to meet the load. This leads to the PV production curtailment of 22% in 2025. Despite this high value, this solution has lower cost than installing more batteries. The curtailment will be reduced as the load increases and Demand Side Management (DSM) techniques can contribute to further reduction by switching part of the load to PV production hours. Potential DSM for the island includes the control of space cooling and refrigerating machines, as well as the control of water supply pumping hours.

B. Frequency Stability Analysis of Optimal Solution

The island grid model of 2025 used the optimized installed generation capacity shown in Table IV.
From the installed 4 diesel units (necessary to cover night peak), 2 units are dispatched during peak PV production so that enough spinning reserve is available. The units are modelled with a power frequency controller which ensures equal active power sharing among these units.
For a total of 8 PV plants, a maximum output of 0,295 MW/plant is used in the simulations. This value takes into consideration that the maximum power output of the entire PV system, given by the inverter rating, is 75% of the total HOMER PV installed capacity.

1) Overview of the PV Frequency Control Response: The response of the generators in the island grid to disturbances, with the PVs participating in frequency regulation, can be seen in Figure 2. The disturbances in the system correspond to a total load variation of 6,5% and an irradiance increase up to 700 W/m^2 followed by a decrease down to 420 W/m^2. The frequency control of the PVs is varying their active power according to the measured frequency disturbances. The PVs will return to their default operation point at the end of the control process. The PVs maximum active power output is limited by the MPP and the default operation point corresponds to a percentage of the MPP. If the frequency variation does not exceed the frequency dead-bands, the PV's droop reaction is not triggered and the diesel generators are the sole to contribute to frequency regulation. From Figure 2, it can be observed that diesel generator and PV's frequency controllers co-exist in the system, without communicating between themselves, and succeed in stabilizing and restoring the frequency.
In a system with a decentralized frequency regulation, it is not possible to adjust the PV's active power output without affecting the frequency. However, by using limited ramping rates in the PVs, the PV output can move gradually towards the new reference value, causing the other generators to adjust their active power accordingly.
The frequency stability analysis performed in the case study aims at determining the system's response when the inertia in the system is at its lowest, thus in high PV penetration events, using high irradiance and load values. In such scenarios, it was observed that the PVs operated below their reserve reference level because the total maximum possible output of the installed PV plants is larger than the maximum demand during daytime (1,8 MW). This situation results in a curtailed PV operation and diesel generators operating at their minimum output power. Because there is no communication between the frequency controllers of the generating units, the PV controller is not aware that the diesel generators are at their minimum limit and will attempt to raise the active power output of the PV to the reference level, causing a small frequency increase. The tests were performed using 10% of the MPP as allocated reserve.
Figure 3 shows the same load event of Figure 2, during a high irradiance scenario (1000 W/m^2). With the diesel generators operating at their minimum output power limit, once the PV output increases towards the reserve level set-point, the frequency becomes larger than the over-frequency dead-band and triggers the control process of the PV, which will stop the active power increase and restore the frequency to nominal. The over-frequency peaks observed due to the attempt to return to the reserve level had an average maximum of 50,73 Hz. Once the control process

[1]Only includes fuel costs, no O&M costs. The total cost is estimated to be 0,21-0,30 EUR/kWh.
[2]Fuel consumption of the 2017 old generators - now decommissioned.

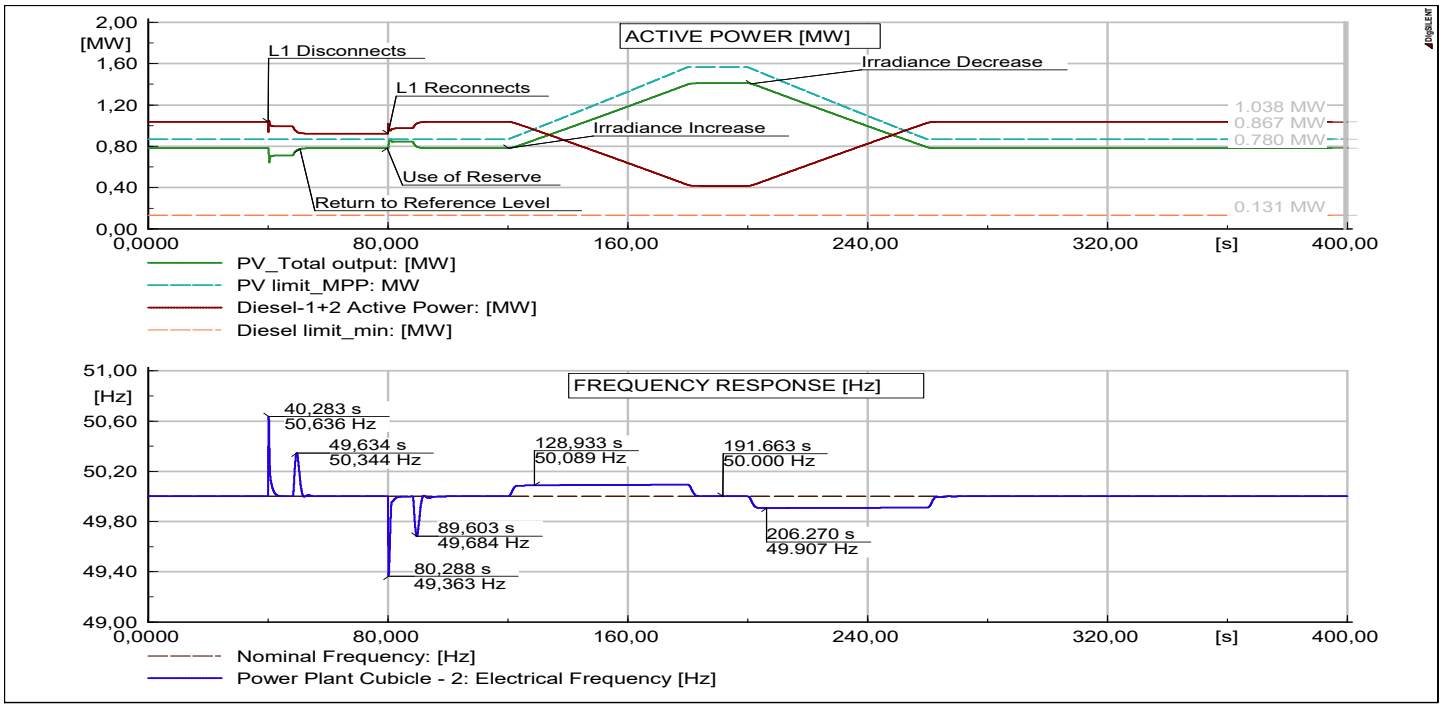

Fig. 2. Overview of the PV participation in frequency regulati

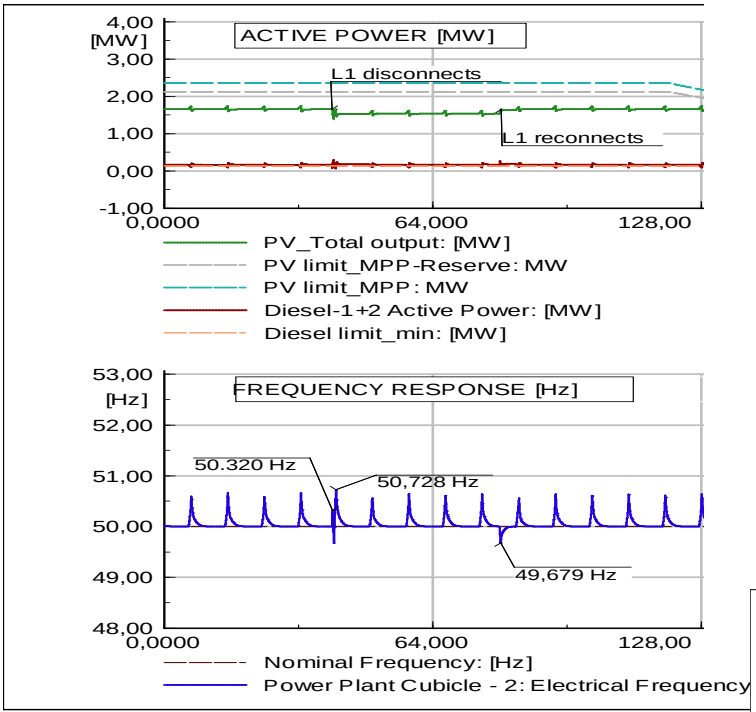

Fig. 3. Overview of the PV participation in frequency regulation during a 6,5% load variation and high irradiance values (1000 W/m^2).

time ends, a new attempt is made by the PV to reach the reserve level. This cycle will repeat itself, resulting in a continuous restarting of the time-based control process, until the PVs can reach their reserve level. This occurs if the reserve level decreases (irradiance decreases) or if the load increases or other generators in the system decrease.

A positive consequence of the operation under a continuous activation of the frequency control process is that if an external event occurs the PV will immediately react. Initially with a milder contribution which will be higher if the frequency exceeds the dead-band limits and activates the contribution using the droop coefficient. A negative consequence of such operation is that the periodic frequency deviations cause a periodic inertial reaction from the diesel generators as shown in Figure 3, observed to be on average ±40 kW from the minimum output level of the diesels. These variations can be reduced by including the battery system proposed in the optimal solution.

2) Comparison of Different PV Frequency Control Operation Modes: During this test, the system response to different modes of operation for the PVs were compared, considering a load variation of 13% and irradiance of 600 W/m^2. The total active power output for the PV and diesel generators can be found in Figures 4 and 5 and the frequency response to the load trip and reconnection can be found in Figure 6.

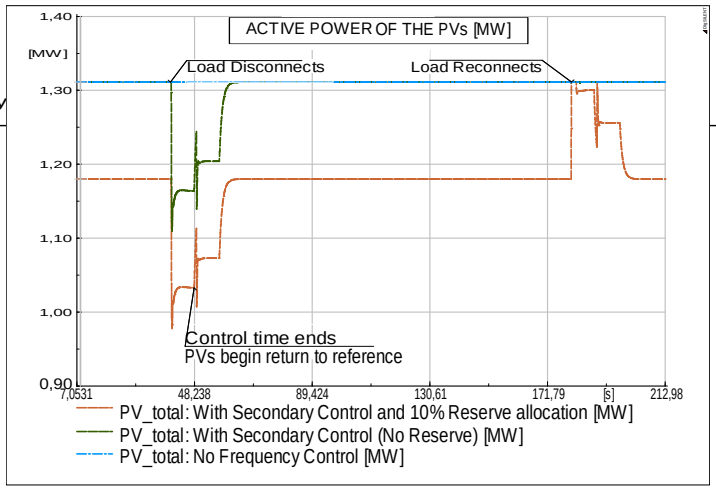

Fig. 4. Total active power output of the PV units under different frequency control modes of operation, during a load variation of 13% and irradiance 600 W/m^2.

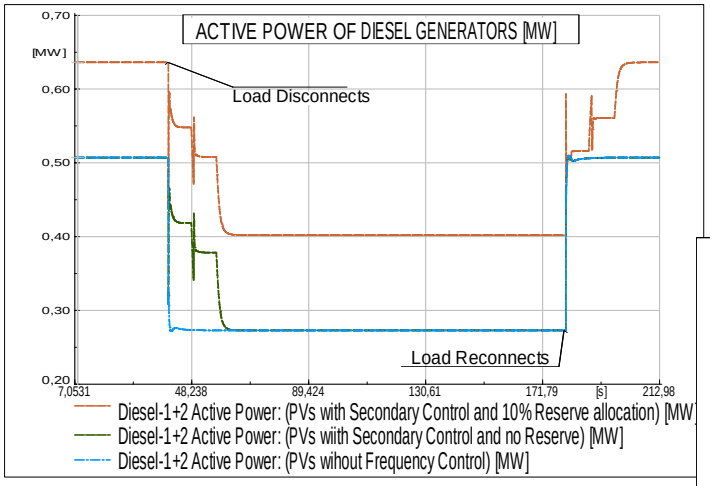

Fig. 5. Total active power output of the diesel generators during PV operation under different frequency control modes, load variation of 13% and irradiance 600 W/m^2.

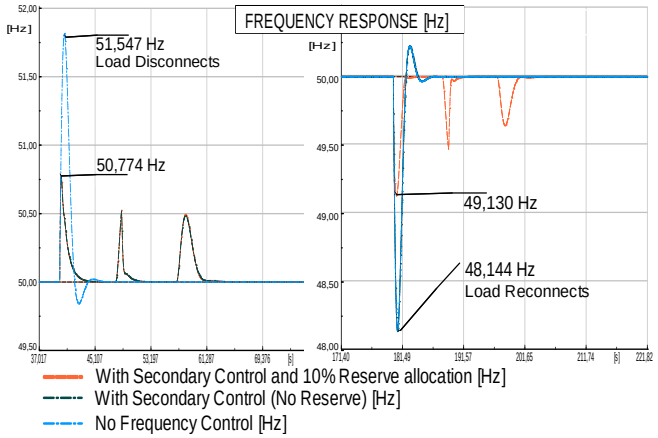

Fig. 6. Frequency response to a 13,5% load disconnection (left) and reconnection (right) and PV operation under different frequency control modes, during irradiance 600 W/m^2.

From Figure 6, it can be concluded that the frequency response is improved when the PVs operate with the proposed controller. The operation of the PVs with a reserve resulted in an improved IFD for the under-frequency event, increasing from 48,14 Hz to 49,13 Hz. For the over-frequency event, the reserve level has no impact on the PV contribution to the frequency regulation as the PVs will reduce their output. The secondary control results with and without reserve yields the same IFD, which is improved when compared to the case in which the PVs have no frequency control, reducing from 51,55 Hz to 50,77 Hz.

When PVs are not being curtailed, the allocation of a reserve power improves the frequency stability of the system, however it results in a higher diesel generation when compared to the scenario in which the PVs operate at their MPP, as seen in Figure 5. When the PVs are being curtailed and operate below the reference level with reserve, the percentage of allocated reserve will not affect the system's frequency response since part of the PV capacity is free, regardless of the reserve setting. Deciding upon which level of reserve to use requires a thorough risk and economic analysis.

3) Irradiance Variation Effect on the Frequency Stability: A cloud movement is simulated, affecting the irradiance received by each PV plant[1]. The active power output of one PV unit of each affected group is shown in Figure 7. The active power in the system per generation type and the frequency response to the event can be seen in Figure 8.

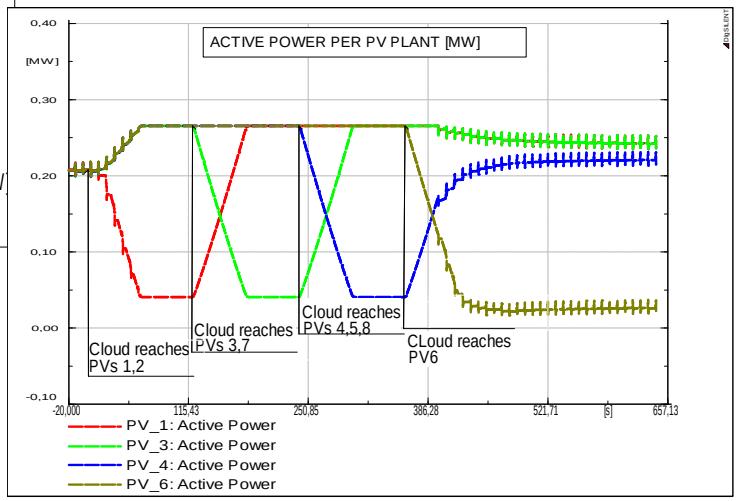

Fig. 7. Active power output per PV plant during irradiance variations simulating a cloud movement.

In this test active power variations of 80% within one minute in simultaneous PV plants resulted in small frequency deviations in the range of 49,96 Hz and 50,05 Hz. Additionally, from Figure 7, it can be observed that after the irradiance variations, the PV plants have different operating points. The last PV plant affected by the cloud coverage (PV 6) remains at a lower active power output. This occurs because when this plant reduces its output, the remaining PV units use this opportunity to increase their output. Due to the high irradiance in the system, when the cloud clears from the last PV plant affected, the system is already optimized with the maximum PV generation (diesels at minimum) and none of the PV plants can further increase their output. This means that PV6 will stay at a lower production level than the others until it has the opportunity to ramp up.

In a dynamic system, the production ratio among the PV plants may continuously vary due to the variation of irradiance received in different plants as well as due to a curtailed operation such as the one shown in Figure 7. This issue is inherent to a system with decentralized secondary control. Overall PV production will always be set to the maximum, but the share between the generators varies. In case of different owners operating the PV systems, it is difficult to ensure equal treatment, however, over time, variations in production between different units will very likely be balanced. On the other hand, in a scenario without curtailment (lower irradiance or higher load) the PVs will reach their reserve level, set as equal among the PV units, and therefore equal active power sharing will be achieved.

[1]Irradiance decrease from 1000 to 200 W/m^2 within 1 minute, with 1 minute of constant 200 W/m^2 input, followed by the increase to 1000 W/m^2 within 1 minute. Total time of the event per plant: 3 minutes. PV plants (1,2); (3,7); (4,5,8); (6) are affected simultaneously.

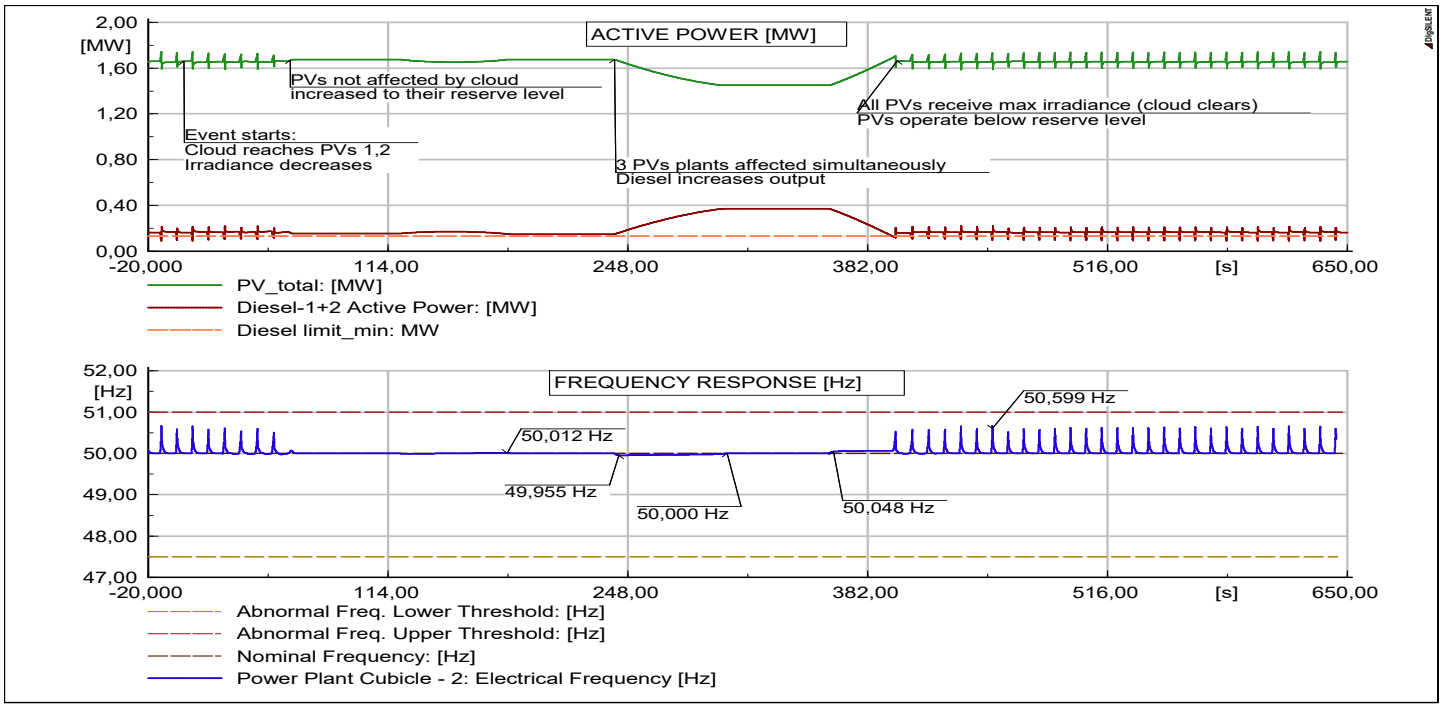

Fig. 8. Active power and frequency response during an irradiance variation in different PV units simulating a cloud movement.

The loss of equal active power sharing among the PV units during a curtailed operation is the consequence of a system without communications. Nevertheless, with the proposed control strategy, the PV's continuous attempt to reach the reserve level guarantees that the total PV output of the system is maximum (diesel at minimum limit), regardless of the active power distribution among the PV units.

4) Frequency Stability Analysis Under a Load Trip and Reconnection Event: The load trip and reconnection of 30,1% of the load during high PV penetration (1000 W/m^2 irradiance) was analyzed. This represents a very extreme load loss, which will cause high IFD not withstood by most protection systems.

An IFD of 52,8 Hz was observed for the over-frequency event, whereas the IFD of 48,8 Hz was observed for the under-frequency event. The frequency remained above the Indonesian grid code's abnormal frequency lower threshold of 47,5 Hz in the under-frequency event, and surpassed the threshold of 51 Hz during 1,9 seconds in the over-frequency event. These values are not applicable to island systems and are mentioned as a reference only. For small island systems with a high share of PVs, the tolerance of the protection setting will be higher than in larger systems. The frequency control coordination with the protection settings in the system must be further analyzed.

5) Frequency Stability Analysis Under a Generator Trip Event: In a first simulation, the system's response to the disconnection of one PV plant is analyzed in a high PV penetration scenario (irradiance of 1000 W/m^2), in which the PV plant supplies 13,7% of the total load's active power. The disconnection of one single PV plant has a small impact on the frequency stability, causing an under-frequency of 49,28 Hz, which is initially compensated by the diesel generators' inertial response and later by the remaining PV plants.

In a second simulation, the effect of a diesel unit disconnection is observed when its generation is higher than the minimum output and it supplies 17,6% of the total load's active power. A scenario with medium PV penetration is used (irradiance of 600 W/m^2). The active power output of the generators at the moment of the disconnection can be found in Figure 9.

When one diesel generator disconnects, the second unit starts to increase its output power, however the frequency decrease soon triggers the PV under-frequency control, raising the PV output to the MPP level and yielding an IFD of 47,4 Hz. The frequency exceeds the abnormal frequency threshold during 0,26 seconds, which is acceptable for an island system. The system remains stable after the loss of one diesel generator, when the remaining diesel unit and PV plants in the system contribute to frequency regulation.

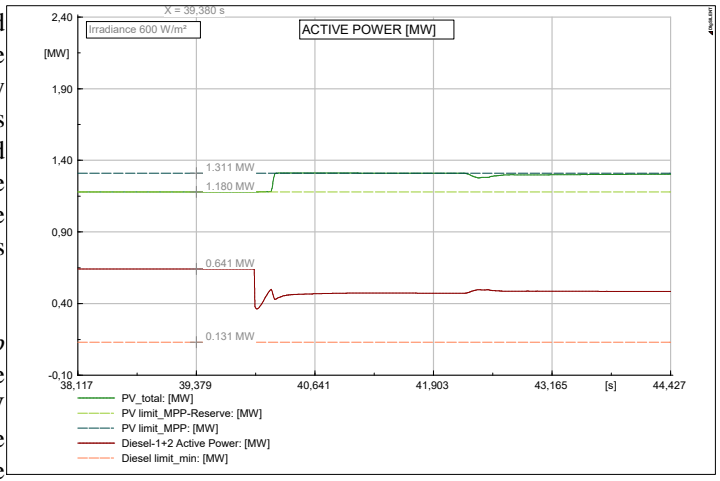

Fig. 9. Active power after the disconnection of one diesel unit, during a medium PV penetration scenario (Irradiance 600 W/m^2).

6) Frequency Stability Analysis Under a Feeder Trip Event: In this test, an entire section of the grid is disconnected during a high PV penetration scenario. The feeder trip caused 0,647 MW of load and 0,508 MW of PV generation to be disconnected, thus causing a small load/generation imbalance and resulting IFD of 50,5 Hz. The results obtained show the importance of the PV distribution across the island grid, located close to large loads. An adequate PV distribution reduces the imbalance and improves the system stability.

IV. Conclusions

The expansion of the installed generation capacity of an island system is optimized, using the tool HOMER Energy Pro. The optimized result meets the 2025 load and renewable energy target with a high penetration of integrated solar photovoltaic generation. The solution with the lowest net present cost of the system is obtained, achieving a significant diesel fuel consumption reduction (19,3%) and cost reduction (19,28%), when compared to a diesel-only system supplying the same load.

The results in Section III-B have confirmed the improvement of the system frequency response when PVs contribute to frequency regulation using the proposed strategy. The technical feasibility of the capacity expansion of an island system using high integration of solar PV generation was validated by the frequency stability analysis. Despite the challenges encountered for operation without communications, the system with the proposed optimal capacity expansion and decentralized control strategy maintains frequency stability under different disturbances in scenarios with a high PV penetration and low inertia and achieves the total maximum PV output in the system even when the PVs have unequal active power sharing. The optimal level of PV allocated reserve must be determined as a balance between the resulting diesel power output level (with corresponding fuel costs and emissions) and the contribution to the frequency regulation (with corresponding IFD and risk of protection tripping and outages). The benefits of the distributed PV generation were observed in Sections III-B3 and III-B6.

The proposed capacity expansion still requires diesel generators. Although these are kept mainly as spinning reserves during high PV production hours, they are the main supply of night load. Demand side management techniques can be applied to switch part of the load to PV production hours and reduce night load and corresponding diesel fuel consumption, as well as PV curtailment and system total costs. A potential solution is to control water supply pumping hours. The technical-economic analysis results can be used as lessons learned in the capacity expansion planning of several similar existing isolated electrical systems. Future developments for this research include: a risk and economic analysis of implementing PVs with different reserve allocations; methods to reduce the effect of frequency deviations caused by the return to the active power reference set-point and the feasibility of having the decentralized method as a backup strategy; economic and technical effects of applying demand side management techniques to the island; further grid integration analysis, including reliability and voltage stability analysis of the proposed system.

References

[1] J. Hernandez, F. Sanchez-Sutil, and P. Bueno, "Large photovoltaic systems providing frequency containment reserves," *Power and Energy Engineering Conference (APPEEC)*, October 2016.

[2] Renewables Ninja, "Renewable energy potential database." https://www.renewables.ninja/, July 2018 [Accessed July 04, 2018].

[3] A. P. Dobos, "NREL PVWatts Manual: PV Derating Factors." https://pvwatts.nrel.gov/downloads/pvwattsv5.pdf, September 2014 [Accessed July 20, 2018].

[4] Reneweconomy, "Solar and PV cost forecast, IRENA forecast and Photon consulting 2016." https://reneweconomy.com.au/solar-and-wind-costs-predicted-to-plunge-by-60-by-2025-24565/, June 2016 [Accessed February 18, 2018].

[5] International Renewable Energy Agency, "Electricity storage and renewables: costs and markets to 2030." http://www.irena.org/-/media/Files/IRENA/Agency/Publication/2017/Oct/IRENA_Electricity_Storage_Costs_2017.pdf, October 2017 [Accessed February 15, 2018].

[6] Secretariat General of the National Energy Council and the Danish Energy Agency, "Technology Data for the Indonesian Power Sector." http://www.ea-energianalyse.dk/reports/1724_technology_data_indonesian_power_ector_dec2017.pdf, December 2017 [Accessed February 15, 2018].

[7] J. Rey, P. Marti, M. J. Velasco, M., and M. Castilla, "Secondary switched control with no communications for islanded microgrids," *IEEE Transactions on Industrial Electronics*, vol. 64(11), pp. 8534–8545, November 2017.

[8] J. Simpson-Porco and F. Dorfler, F.and Bullo, "Synchronization and power sharing for droop-controlled inverters in islanded microgrids," *IEEE Transactions on Industrial Electronics*, vol. 49(9), pp. 2603–2611, September 2013.

[9] Grid Modernization Laboratorium Consortium, US Department of Energy, "The frequency-watt function: Simulation and testing for the hawaiian electric companies." https://www.nrel.gov/docs/fy17osti/68884.pdf, July 2017 [Accessed April 06, 2018].